

Crystal structures of natural ternary apatites: Solid solution in the $\text{Ca}_5(\text{PO}_4)_3\text{X}$ ($\text{X} = \text{F}, \text{OH}, \text{Cl}$) system

JOHN M. HUGHES, MARYELLEN CAMERON, KEVIN D. CROWLEY

Department of Geology, Miami University, Oxford, Ohio 45056, U.S.A.

ABSTRACT

The crystal structures of $P6_3/m$ ternary apatite [$\text{Ca}_5(\text{PO}_4)_3(\text{F}_{0.39}\text{Cl}_{0.33}\text{OH}_{0.28})$] and a previously unrecognized $P2_1/b$ ternary apatite [$\text{Ca}_5(\text{PO}_4)_3(\text{F}_{0.29}\text{Cl}_{0.47}\text{OH}_{0.24})$; $b = 2a$, $\gamma = 120^\circ$] were refined to R values of 0.015 and 0.047, respectively, using three-dimensional X-ray data. Phosphate tetrahedra and Ca(1) polyhedra of both structures are generally very similar to analogous polyhedra in the end-member fluor-, chlor-, and hydroxylapatite structures. The Ca(2) polyhedron, which includes among its ligands the column anions, exhibits significant but regular variations in interatomic distances that can be directly correlated to Cl content.

Solid solution in hexagonal ternary apatite is achieved by a 0.4-Å shift along c of the Cl atom relative to its position in end-member chlorapatite. This adjustment affects a Markovian sequence of anions in the (0, 0, z) anion columns by providing a structural environment that includes column OH species at a distance of 2.96 Å from Cl. The shift of the Cl atom is accompanied by splitting of the Ca(2) atoms into two distinct positions as a function of the kind of anion neighbor (F or OH vs. Cl). An additional nonequivalent Cl site, similar to that in end-member chlorapatite, is also present. Those Cl atoms with adjacent OH occupy a site different from Cl atoms adjacent to vacancies in the anion column.

The reduction of symmetry in monoclinic ternary apatite results from the ordering of Cl and OH within the anion columns. The atomic positions of Cl and OH in the anion column are equivalent to those in hexagonal ternary apatite, but each is ordered into only one of the two hexagonal symmetry-equivalent sites.

INTRODUCTION

Like those of many common minerals, crystal structure studies of calcium phosphate apatites [$\text{Ca}_5(\text{PO}_4)_3\text{X}$; ($\text{X} = \text{F}, \text{OH}, \text{Cl}$)] were long ago considered complete. The hexagonal $P6_3/m$ structure was determined 60 years ago (Náray-Szabó, 1930; Mehmel, 1930), and more recent refinements on end-members in the ternary system have illustrated monoclinic variants of the basic apatite structure (chlorapatite: e.g., Mackie et al., 1972; Hounslow and Chao, 1970; hydroxylapatite: e.g., Elliot et al., 1973). Detailed structure descriptions and polyhedral arrangements are illustrated by Beevers and McIntyre (1946) and Hughes et al. (1989).

Interest among geologists in the apatite minerals has increased in recent years. Petrologists have proposed that the F, OH, and Cl variations in calcium phosphate apatites are potential geothermometers (e.g., Stormer and Carmichael, 1971) and indicators of P activity and volatile fugacity in magmatic, metamorphic, and hydrothermal processes (e.g., Yardley, 1985; Candela, 1986; Boudreau and McCallum, 1987; Morrison and Valley, 1989). Apatite is among the most important rare-earth element-bearing phases in igneous rocks (e.g., Henderson, 1984), and its role in crustal anatexis, granitoid production, and

mantle enrichment was addressed in studies by Harrison and Watson (1984), Watson et al. (1985), and Exley and Smith (1982). Other recent studies have shown that F, OH, and Cl concentrations correlate with etching rates and annealing properties of U fission tracks in apatites (Green et al., 1986; Crowley and Cameron, 1987; Crowley et al., 1988; Crowley and Cameron, unpublished manuscript). The apatite structure has also received attention as a host phase for long-lived actinides in nuclear waste formulations (e.g., Weber et al., 1985; Weber and Roberts, 1983).

Recent experiments in our laboratory demonstrate that many fundamental aspects of the apatite atomic arrangement are not well understood, including mechanisms of ternary solution in natural crystals. In this study of ternary apatites we describe the crystal structures of hexagonal ternary apatite and a previously unrecognized monoclinic variant of the ternary apatite structure.

EXPERIMENTAL DETAILS

Hexagonal ternary apatite

Hexagonal ternary F-OH-Cl apatite was represented by a specimen collected from "ash F" in the Gunnison Formation near Jackson Peak, southwestern Utah (Nielson,

TABLE 1. Experimental data for hexagonal and monoclinic ternary apatites

	Hexagonal	Monoclinic
Size	Elliptical, 0.13 × 0.13 × 0.16 mm	Approx. tetrahedron, 0.35 mm on edge
Cell parameters		
Least squares		
<i>a</i> (Å)	9.459(2)	9.488(6)
<i>b</i>	9.464(2)	18.963(9)
<i>c</i>	6.849(2)	6.822(5)
α (°)	90.03(2)	90.00(5)
β	89.98(2)	89.93(6)
γ	119.99(1)	119.97(5)
Idealized		
<i>a</i> (Å)	9.4615	9.4877
<i>b</i>	—	18.9628
<i>c</i>	6.8491	6.8224
γ (°)	—	119.9739
Radiation	MoK α , Zr filter	MoK α , graphite monochromated
Theta range	0–26°	0–26°
No. of reflections	1206	4172
Absorption correction	psi scans	psi scans, DIFABS
Unique reflections	386	2090
R_{merge}	0.014	0.030
Reflections with $I > 3\sigma_I$	307	—
<i>R</i>	0.015	0.047
R_w	0.025	0.043
$\Delta\rho$ residual (e/Å ³)		
(+)	0.202	0.910
(–)	0.362	0.594

Note: For Table 1 and subsequent tables, numbers in parentheses denote one esd of least significant figure.

1988); crystal abrasion during airborne transport of the ash yielded rounded, nearly spherical crystals. Composition of the crystals was determined by electron probe microanalysis with the Southern Methodist University JEOL SUPERPROBE using well-analyzed standards. (Full details of analysis are available from the authors.) Analysis of the Gunnison sample yielded (Ca_{4.96}Mn_{0.01}Fe_{0.02}Sr_{0.01}Na_{0.02}Ce_{0.01})_{Σ5.03}(P_{2.94}Si_{0.02}S_{0.02})_{Σ2.98}O₁₂(F_{0.39}Cl_{0.33}OH_{0.28})_{Σ1.00}, with OH determined by difference. For structure refinement the composition was assumed to correspond to pure calcium phosphate apatite, with column-anion composition as determined by microprobe analysis.

TABLE 2. Positional parameters and equivalent isotropic temperature factors, *B* (Å²) for hexagonal ternary apatite

Atom	<i>x</i>	<i>y</i>	<i>z</i>	<i>B</i> (Å ²)
Ca(1)	2/3	1/3	0.0018(1)	0.98(1)
Ca(2) _A	–0.00699(9)	0.23861(9)	1/4	0.64(2)
Ca(2) _B	–0.0018(2)	0.2709(2)	1/4	0.60(3)
P	0.36968(8)	0.40053(8)	1/4	0.68(1)
O(1)	0.4862(2)	0.3315(2)	1/4	1.08(4)
O(2)	0.4651(2)	0.5884(2)	1/4	1.42(5)
O(3)	0.2597(2)	0.3450(2)	0.0699(3)	1.68(3)
F	0	0	1/4	1.93
O(H)	0	0	0.200(3)	1.31
Cl _B	0	0	0.368(2)	2.68
Cl _A	0	0	0.44(1)	2.68

Note: Subscripts A and B refer to positions for the split atoms.

TABLE 3. Anisotropic thermal parameters (× 10⁴) for atoms in hexagonal ternary apatite

Atom	β_{11}	β_{22}	β_{33}	β_{12}	β_{13}	β_{23}
Ca(1)	41.7(6)	41.7	37(2)	41.7	0	0
Ca(2) _A	27.1(8)	13.2(8)	42(2)	18(1)	0	0
Ca(2) _B	32(2)	2(2)	37(3)	6(2)	0	0
P	25.8(7)	27.1(7)	38(1)	32(1)	0	0
O(1)	43(2)	55(2)	57(4)	73(3)	0	0
O(2)	52(2)	30(2)	110(5)	43(3)	0	0
O(3)	52(2)	106(2)	68(3)	106(2)	–52(4)	–81(5)
F	29	29	220	29	0	0
O(H)	30	30	120	30	0	0
Cl _B	56	56	270	56	0	0
Cl _A	56	56	270	56	0	0

Note: The form of the anisotropic displacement parameter is $\exp[-(\beta_{11} \cdot h^2 + \beta_{22} \cdot k^2 + \beta_{33} \cdot l^2 + \beta_{12} \cdot hk + \beta_{13} \cdot hl + \beta_{23} \cdot kl)]$.

Precession *a*- and *b*-axis photographs confirmed the absence of monoclinic superstructure reflections and yielded diffraction effects consistent with space group *P6₃/m*. Intensity data used for structure refinement were measured with an Enraf-Nonius CAD-4 diffractometer. Table 1 summarizes the details of data collection and refinement.

All crystal structure calculations were undertaken in space group *P6₃/m* using the SDR package of computer programs (Frenz, 1985), employing neutral-atom scattering factors with terms for anomalous dispersion. Starting parameters were taken from fluorapatite (Hughes et al., 1989), and column-anion positions were initially located using difference maps. Fluorine was fixed in the mirror plane at (0, 0, 1/4), and difference maps supported the validity of this assumption. The thermal parameters of F, O(H), and Cl were fixed at the values of the hexagonal end-members (Hughes et al., 1989), and an isotropic extinction factor was refined. No attempt was made to locate the H atom because of its low concentration.

Full-matrix, least-squares refinement was undertaken using data with $I > 3\sigma_I$ and structure factors weighted proportional to σ_I^{-2} , with a term to downweight intense reflections. Initial refinement was undertaken assuming single sites for Ca(2) and Cl, and the refinement converged at $R = 0.017$. Refined thermal parameters of Ca(2) supported imposition of the disordered Ca(2) model of Sudarsanan and Young (1978). In this split-site model Ca(2)_B occupancy was constrained to be equal to Cl occupancy. With the two Ca(2) positions the structure refined routinely, including anisotropic thermal parameters for both Ca(2) sites, to $R = 0.015$. Thermal parameters of the Cl ion were then released to assess any site disordering (values were subsequently fixed as noted above). The U_{33} value of the Cl atom refined to an unusually large value of 0.098 Å², suggesting disordering of the Cl. The site was then split and multiplicities of both sites were refined. The refinement converged at $R = 0.015$, and the sum of the multiplicities of the two chlorine sites converged at 0.63 atoms per unit cell, vs. 0.66 as determined by microprobe. The significance of the split Cl atoms is discussed in a later section. Examination of bond lengths showed one

unusually short Ca(2)_B-O(2) bond (2.16 Å), suggesting that the Ca(2) disorder propagates to disorder O(2). The thermal parameters of O(2) support this positional disorder, but a split O(2) model was not invoked.

Table 2 contains positional parameters and equivalent isotropic B values for all atoms, and Table 3 presents anisotropic thermal parameters. Table 4 lists selected bond lengths and tetrahedral bond angles for hexagonal ternary apatite, and Table 5¹ gives observed and calculated structure factors.

Monoclinic ternary apatite

Monoclinic ternary apatite was found in a split of material from which monoclinic chlorapatite was first described (Hounslow and Chao, 1970). The crystal selected was a pale pink crystal thought to represent monoclinic chlorapatite. The crystal was mounted and oriented for precession studies (MoK α radiation). Photographs taken with *c** (monoclinic first setting for comparison with the hexagonal apatite cell) as the goniometer head axis displayed a superstructure along one of the pseudohexagonal *a*-axes (Fig. 1); comparison of lattice parameters and intensities of the superstructure reflections with those of monoclinic chlorapatite (Hounslow and Chao, 1970) demonstrated that the material was not monoclinic chlorapatite. Microprobe analysis undertaken after data col-

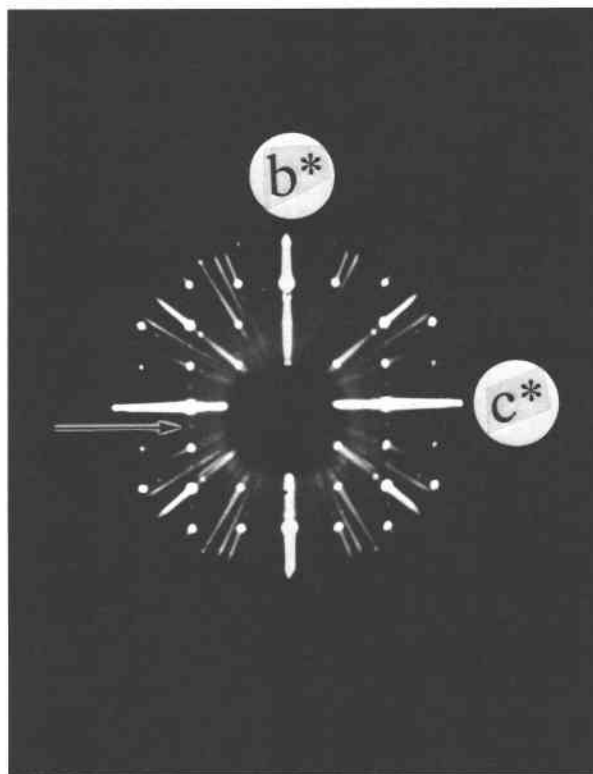


Fig. 1. Precession photograph (*a* axis, 0-level) of monoclinic ternary apatite. Superstructure reflections (example denoted by arrow) exist as ($k = 2n + 1, l \neq 0$). MoK α radiation, Zr filter, 4.0 h.

¹ Copies of Tables 5, 8, and 9 may be ordered as Document AM-90-428 from the Business Office, Mineralogical Society of America, 1625 I Street, N.W., Suite 414, Washington, D.C. 20006, U.S.A. Please remit \$5.00 in advance for the microfiche.

TABLE 4. Selected bond lengths (Å) and tetrahedral bond angles (°) for hexagonal ternary apatite

Ca(1) ^A -O(1) ^{A,B,C}	2.403(2)		
-O(2) ^{D,E,F}	2.450(2)		
-O(3) ^{D,E,F}	2.806(2)		
Mean	2.553		
Ca(2) _A -O(1) ^B	2.761(2)		
-O(2) ^C	2.433(2)		
-O(3) ^{A,J}	2.522(2)		
-O(3) ^{F,I}	2.353(2)		
-F ^A	2.2913(9)		
-O(H) ^A	2.317(3)		
-Cl _A	2.63(4)		
Mean _{oxy}	2.491		
Ca(2) _B -O(1) ^B	2.741(2)		
-O(2) ^C	2.164(2)		
-O(3) ^{A,J}	2.530(2)		
-O(3) ^{F,I}	2.314(2)		
-Cl _B	2.695(4)		
Mean _{oxy}	2.432		
P ^A -O(1) ^A	1.537(3)		
-O(2) ^A	1.540(2)		
-O(3) ^{A,J}	1.528(2)		
Mean	1.533		
O(1) ^A -P ^A -O(2) ^A	111.06(12)	O(2) ^A -P ^A -O(3) ^A	107.62(9)
O(1) ^A -P ^A -O(3) ^A	111.34(9)	O(3) ^A -P ^A -O(3) ^J	107.69(9)

^A = *x, y, z*, Table 2; ^B = $-y, x - y, z$; ^C = $y - x, -x, z$; ^D = $-x, -y, -z$; ^E = $y, y - x, -z$; ^F = $x - y, x, -z$; ^G = $-x, -y, 1/2 + z$; ^H = $y, y - x, 1/2 + z$; ^I = $x - y, x, 1/2 + z$; ^J = $x, y, 1/2 - z$; ^K = $-y, x - y, 1/2 - z$; ^L = $y - x, -x, 1/2 - z$.

TABLE 6. Positional parameters and equivalent isotropic B (\AA^2) for monoclinic ternary apatite

Atom	x	y	z	B
Ca(1) _I	0.3313(1)	0.58243(5)	0.0020(1)	1.14(2)
	$\frac{1}{2}$	0.58333	0.0018	
Ca(1) _{II}	0.3356(1)	0.58434(5)	0.4980(2)	1.51(2)
	$\frac{1}{2}$	0.58333	0.4982	
Ca(2) _I	0.2511(1)	0.24809(5)	0.2498(2)	1.48(2)
	0.24887	0.24739	$\frac{1}{4}$	
Ca(2) _{II}	-0.0038(1)	0.62258(6)	0.7492(2)	1.48(2)
	-0.00523	0.62295	$\frac{3}{4}$	
Ca(2) _{III}	0.2550(1)	0.37554(5)	0.7503(2)	1.49(2)
	0.25410	0.37444	$\frac{3}{4}$	
P _I	0.4018(1)	0.43534(6)	0.2505(2)	1.01(2)
	0.40053	0.43484	$\frac{1}{4}$	
P _{II}	0.6292(1)	0.26557(6)	0.2508(2)	1.02(2)
	0.63032	0.26543	$\frac{1}{4}$	
P _{III}	0.0312(1)	0.45093(6)	0.7502(2)	1.02(2)
	0.03085	0.45027	$\frac{3}{4}$	
O(1) _I	0.3346(3)	0.4939(2)	0.2510(5)	1.41(6)
	0.3315	0.4931	$\frac{1}{4}$	
O(1) _{II}	0.4880(4)	0.3268(2)	0.7511(5)	1.41(7)
	0.4862	0.3274	$\frac{3}{4}$	
O(1) _{III}	0.1534(3)	0.5829(2)	0.2492(5)	1.41(7)
	0.1547	0.5843	$\frac{1}{4}$	
O(2) _I	0.5894(4)	0.4825(2)	0.2465(6)	1.63(7)
	0.5884	0.4826	$\frac{1}{4}$	
O(2) _{II}	0.5346(4)	0.3121(2)	0.2490(6)	1.62(7)
	0.5349	0.3117	$\frac{1}{4}$	
O(2) _{III}	0.1242(4)	0.5447(2)	0.7476(6)	1.60(7)
	0.1233	0.5442	$\frac{3}{4}$	
O(3) _I	0.3441(4)	0.3800(2)	0.0709(6)	2.00(7)
	0.3450	0.3799	0.0699	
O(3) _{II}	0.7399(4)	0.2926(2)	0.7010(6)	1.89(8)
	0.7403	0.2927	0.0699	
O(3) _{III}	0.0846(4)	0.4217(2)	0.5710(6)	1.93(7)
	0.0853	0.4225	0.5699	
O(3) _{IV}	0.3508(4)	0.3817(2)	0.4331(6)	2.00(7)
	0.3450	0.3799	0.4301	
O(3) _V	0.7365(4)	0.2932(2)	0.4329(6)	2.10(8)
	0.7403	0.2927	0.4301	
O(3) _{VI}	0.0865(4)	0.4258(2)	0.9338(6)	2.05(8)
	0.0853	0.4225	0.9301	
Cl _B	-0.000(1)	0.2507(6)	0.130(2)	1.39(20)
	0	$\frac{1}{4}$	0.132	
Cl _A	-0.0000(5)	0.2494(2)	0.4345(7)	1.22(6)
	0	$\frac{1}{4}$	0.44	
F	0.0000(8)	0.2502(4)	0.237(1)	1.40(10)
	0	$\frac{1}{4}$	$\frac{1}{4}$	
O(H)	0.0006(8)	0.2498(4)	0.340(1)	0.14(10)
	0	$\frac{1}{4}$	0.30	

Note: For all atoms, the atomic coordinates in the second row are calculated from the parameters of equivalent atoms in hexagonal ternary apatite [without disordered Ca(2)] with appropriate transformation to the cell for $P2_1/b$.

* Roman numeral subscripts designate monoclinic, symmetrically degenerate equivalents of hexagonal atoms.

lection confirmed that the crystal was a F-, OH-, Cl-bearing ternary apatite. Microprobe analysis yielded the formula $\text{Ca}_{5.05}(\text{P}_{3.00}\text{Si}_{0.03})_{\Sigma 3.03}\text{O}_{12}(\text{F}_{0.29}\text{OH}_{0.24}\text{Cl}_{0.47})_{\Sigma 1.00}$, with OH obtained by difference.

Prior to structure analysis we realized that the crystal, the only one isolated to date, was not of ideal quality for a high-precision X-ray structure study. Abundant inclusions (~3–4 vol%) and the large crystal size precluded a superior refinement, but the unique nature of the preliminary data prompted further study.

The crystal was mounted on an Enraf-Nonius CAD-4 diffractometer. Lattice parameters were refined (no sym-

metry constraints) using diffraction angles from 25 automatically centered reflections (Table 1). The cell was defined with c as the unique monoclinic axis and b as the superstructure axis; thus $b = 2a$. Results of the cell refinement and details of three-dimensional data collection are presented in Table 1.

The data set and precession photographs were examined for systematic extinctions; refinement was initiated in space group $P2_1/b$ because of the absence of $hk0$, $k = 2n + 1$ reflections and by analogy to other monoclinic apatites. The zero-moment test yielded an intensity distribution not inconsistent with the centrosymmetric space group. Subsequent successful refinement in $P2_1/b$ (and unsuccessful refinement in $P2_1$ and Pb) supported the choice of space group.

Full-matrix least-squares refinement was initiated using the atomic positions for Ca, P, and O in $P2_1/b$ chlorapatite (Mackie et al., 1972). During early stages of refinement, no column anions were included and isotropic B values were fixed. After initial refinement, equivalent data were averaged and isotropic thermal parameters were refined. The R value converged at 0.146 without addition of column anions. A difference map then revealed that the four largest peaks were near $(0, \frac{1}{4}, z)$, which are equivalent to $(0, 0, z)$ positions in space group $P6_3/m$. Based on the bond distance to Ca(2), one site was assigned to Cl and the other three were modeled with F scattering factors to represent the iso-electronic F and O ions. Occupancy was refined, and fixed isotropic B values of F = 1.0 and Cl = 1.5 \AA^2 were assigned. The R value converged at 0.081, and a difference map revealed no missing atoms.

The psi-scan-corrected data were further adjusted using the program DIFABS of Walker and Stuart (1983). After re-averaging data and refining all atoms except column anions in the anisotropic mode, $R = 0.049$.

Comparison of positions of the column anion sites with those in hexagonal ternary apatite suggested that one site assigned to O and/or F in the early stages of refinement was equivalent to a chlorine position in hexagonal ternary apatite. After assigning Cl to that position and further refining the structure by alternatively refining column-anion occupancy and isotropic thermal parameters, R converged at 0.047. The data did not support anisotropic thermal-parameter refinement for column anions. In the final refinement with isotropic temperature factors for the column anions, the B value of the column hydroxyl oxygen refined to an atypically low value (0.14 \AA^2). Anion occupancy converged at Cl = 0.37, F = 0.38, and O(H) = 0.29 atoms per formula unit, compared to Cl = 0.47, F = 0.29 and O(H) = 0.24 atoms per formula unit by microprobe. The differences are attributed to the inferior quality of the crystal; difference maps showed no unusual peaks in the anion columns.

A zero-sigma cutoff and unit weights for all reflections were used throughout all refinement cycles. The data set essentially consists of two groups of reflections, the very weak superstructure reflections and the strong "hexagonal apatite" reflections. Exhaustive experimentation with var-

TABLE 7. Bond lengths (Å) and tetrahedral bond angles (°) for atoms in monoclinic ternary apatite

Ca(1) _i -O(1) _i	2.400(4)	Ca(1) _i -O(1) _i	2.402(4)
-O(1) _{ii}	2.407(3)	-O(1) _{ii}	2.390(3)
-O(1) _{iii}	2.390(4)	-O(1) _{iii}	2.413(4)
-O(2) _i	2.425(4)	-O(2) _i	2.461(4)
-O(2) _{ii}	2.452(3)	-O(2) _{ii}	2.437(4)
-O(2) _{iii}	2.445(4)	-O(2) _{iii}	2.446(4)
-O(3) _i	2.837(4)	-O(3) _{iii}	2.845(3)
-O(3) _{ii}	2.814(5)	-O(3) _{iv}	2.752(4)
-O(3) _{vi}	2.746(3)	-O(3) _v	2.769(5)
Mean	2.546	Mean	2.546
Ca(2) _i -O(1) _{iii}	2.788(4)	Ca(2) _i -O(1) _i	2.793(3)
-O(2) _{ii}	2.334(3)	-O(2) _{iii}	2.333(4)
-O(3) _i	2.514(4)	-O(3) _{ii}	2.518(3)
-O(3) _{iii}	2.339(4)	-O(3) _{iii}	2.328(4)
-O(3) _{iv}	2.546(4)	-O(3) _v	2.545(3)
-O(3) _v	2.322(4)	-O(3) _{vi}	2.327(4)
-Cl _B	2.542(12)	-Cl _B	2.53(1)
-Cl _A	2.706(5)	-Cl _A	2.717(5)
-F	2.404(9)	-F	2.397(9)
-O(H)	2.471(9)	-O(H)	2.482(9)
Mean _{oxy}	2.474	Mean _{oxy}	2.474
Ca(2) _{iii} -O(1) _{ii}	2.791(4)		
-O(2) _i	2.335(3)		
-O(3) _i	2.332(4)		
-O(3) _{iii}	2.507(4)		
-O(3) _{iv}	2.328(4)		
-O(3) _{vi}	2.559(5)		
-Cl _B	2.544(8)		
-Cl _A	2.705(4)		
-F	2.404(6)		
-O(H)	2.479(6)		
Mean _{oxy}	2.475		
P _i -O(1) _i	1.532(4)	P _{ii} -O(1) _{ii}	1.535(3)
-O(2) _i	1.542(3)	-O(2) _{ii}	1.540(4)
-O(3) _i	1.526(4)	-O(3) _{ii}	1.527(4)
-O(3) _{iv}	1.526(4)	-O(3) _v	1.524(4)
Mean	1.532	Mean	1.532
O(1) _i -P _i -O(2) _i	110.93(18)	O(1) _{ii} -P _{ii} -O(2) _{ii}	110.84(18)
O(1) _i -P _i -O(3) _i	111.35(22)	O(1) _{ii} -P _{ii} -O(3) _{ii}	111.62(20)
O(2) _i -P _i -O(3) _{iv}	111.90(22)	O(1) _{ii} -P _{ii} -O(3) _v	111.72(21)
O(2) _i -P _i -O(3) _{iii}	107.37(21)	O(2) _{ii} -P _{ii} -O(3) _{ii}	107.54(23)
O(2) _i -P _i -O(3) _v	106.93(21)	O(2) _{ii} -P _{ii} -O(3) _v	106.83(23)
O(3) _i -P _i -O(3) _{iv}	108.15(19)	O(3) _{ii} -P _{ii} -O(3) _v	108.06(20)
P _{iii} -O(1) _{iii}	1.535(3)		
-O(2) _{iii}	1.541(3)		
-O(3) _{iii}	1.530(4)		
-O(3) _{vi}	1.524(4)		
Mean	1.533		
O(1) _{iii} -P _{iii} -O(2) _{iii}	110.97(21)		
O(1) _{iii} -P _{iii} -O(3) _{iii}	111.48(19)		
O(1) _{iii} -P _{iii} -O(3) _{vi}	111.54(19)		
O(2) _{iii} -P _{iii} -O(3) _{iii}	107.88(19)		
O(2) _{iii} -P _{iii} -O(3) _{vi}	106.42(20)		
O(3) _{iii} -P _{iii} -O(3) _{vi}	108.34(24)		

ious weighting schemes and cutoff values demonstrated that their use biased the data set against the weaker superstructure reflections, and thus unit weights for all reflections were used. This choice of refinement parameters may affect the final *R* value and thermal parameters, but it does not bias the data set nor ultimately the positional parameters against the superstructure reflections.

Table 6 presents positional parameters and isotropic thermal parameters for all atoms in the structure, and Table 7 gives selected bond lengths and tetrahedral bond angles for the structure. Table 8 (see footnote 1) presents anisotropic thermal parameters for all cations and oxygen

atoms [except O(H)], and Table 9 (see footnote 1) gives observed and calculated structure factors.

CONFIGURATION OF ANION COLUMNS AND MECHANISMS OF SOLID SOLUTION

Hexagonal variants

In end-member hexagonal apatite structures the positions of column anions are not constrained by unlike anion species in the [0, 0, *z*] anion columns. Thus the column anions occur at sites that result in the ideal bond distance to the trigonally disposed Ca(2) atoms in the mirror planes

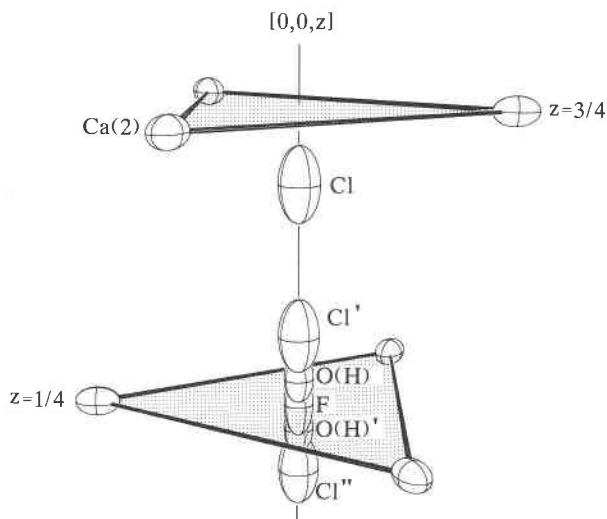


Fig. 2. Depiction of possible anion positions in the hexagonal ternary apatite structure. Stippled planes represent mirror planes at $z = 1/4, 3/4$, each containing a triangle of Ca(2) atoms (connected by "bonds"). Atom Cl represents a Cl atom disordered below the mirror plane at $z = 3/4$, and other column anions represent the five possible anion neighbors associated with the mirror plane at $z = 1/4$ (Cl' = Cl disordered above that plane; O(H) = OH oxygen disordered above that plane; F = fluorine atom at $0, 0, 1/4$; and O(H)' and Cl'' represent OH oxygen and Cl atoms disordered below the mirror plane at $z = 1/4$).

at $z = 1/4, 3/4$ (Fig. 2). In hexagonal fluorapatite, the F atoms lie in the plane of the mirrors at the center of the Ca(2) triangles. In hexagonal hydroxylapatite, the OH ions are displaced from the Ca(2) triangle and occupy disordered, mirror-related sites near $(0, 0, 0.20)$ and $(0, 0, 0.30)$ [and $(0, 0, 0.70)$ and $(0, 0, 0.80)$], each half-occupied. Like OH, the larger Cl atoms in chlorapatite are also displaced from the centers of the Ca(2) triangles and are disordered between mirror-related sites near $(0, 0, 0.43)$ and $(0, 0, 0.07)$ [and $(0, 0, 0.93)$ and $(0, 0, 0.57)$] that are 1.2 \AA from the plane.

The three hexagonal end-member anion columns are incompatible in solid solution. Figure 2 depicts an example of a Cl atom (the atom labeled Cl in Fig. 2) located at the Cl position ($z = 0.57$) disordered below the mirror plane at $z = 3/4$. For that particular Cl atom, possible column-anion neighbors associated with the adjacent mirror plane at $z = 1/4$ are (1) a Cl located above the $z = 1/4$ plane (Cl-Cl' distance = 0.92 \AA), (2) an OH ion disordered above the mirror plane [Cl-O(H) distance = 1.81 \AA], (3) an F ion in the plane of the mirror at $(0, 0, 1/4)$ (Cl-F distance = 2.16 \AA), (4) a OH ion disordered below the mirror plane [Cl-O(H)' distance = 2.51 \AA], and (5) a Cl ion disordered below the $z = 1/4$ mirror plane (Cl-Cl'' distance = $c/2 = 3.4 \text{ \AA}$). On the basis of anion positions in the hexagonal end-member structures, all of these anion neighbors for the Cl ion except Cl'' are prohibited based on anion-anion distances. It is thus not immediately ap-

parent how solid solution is achieved in hexagonal ternary apatite. The structure refinement of hexagonal ternary apatite described below demonstrates that one mechanism that enables solid solution in *hexagonal* ternary apatites involves a 0.4 \AA shift of the Cl atom toward its associated mirror plane, relative to the Cl position in end-member chlorapatite. This structural adjustment allows an OH neighbor at the OH position near the adjacent mirror plane.

Anions in the $[0, 0, z]$ columns are located at different positions in end-member and ternary apatite structures. In hexagonal end-member chlorapatite, the Cl atom is unfettered by adjacent non-Cl anions in the $[0, 0, z]$ columns, and the atom half-occupies a position at $(0, 0, 0.5677)$ about the $z = 3/4$ mirror plane. In hexagonal *ternary* apatite, however, the Cl atom position shifts in response to the presence of non-Cl anion neighbors. The Cl response involves a shift of 0.4 \AA closer to the $z = 3/4$ mirror plane, to a half-occupied $(0, 0, 0.632)$ position. This shift in Cl position results in an atomic arrangement that accommodates an OH neighbor at the OH position disordered below the adjacent plane at $z = 1/4$ [O(H)' in Fig. 2]. The Cl-O distance is a reasonable 2.96 \AA , compared with 2.52 \AA calculated with anion positions in the hexagonal end-member chlor- and hydroxylapatite structures.

Associated with the shift of the Cl position is splitting of the single Ca(2) site into two disordered sites. In a structure refinement of another ternary apatite, Sudarsanan and Young (1978) demonstrated that the shift of the Cl atoms closer to the Ca(2) triangles causes a portion of the Ca(2) atoms (a portion equivalent to Cl concentration) to disorder to a new position to maintain the ideal Ca-Cl bond distance (ca. 2.70 \AA). Two Ca(2) positions thus result: Ca(2)_A, in which Ca(2) atoms bond to F or OH species, and Ca(2)_B, in which Ca bonds to the Cl_B atoms. An added complication not recognized in the Sudarsanan and Young sample is evident, however, in two sets of split sites observed for the Cl ion in our sample.

As noted previously, thermal parameters of the Cl ion in our refinement suggested split Cl sites. Upon splitting of the Cl into two sites, the positions of the split atoms refined to those of Cl_B [ca. $(0, 0, 0.37)$], the "normal" ternary apatite Cl position constrained by a OH and by bonding to Ca(2)_B and Cl_A [ca. $(0, 0, 0.44)$], a Cl position adjacent to a vacancy. [As shown by Sudarsanan et al. (1977) and Wilson et al. (1977), vacancies commonly occur in apatite anion columns.] The Cl_A position bonds to Ca(2)_A, and is identical to the Cl position in hexagonal end-member chlorapatite, as in both cases the Cl is unfettered by unlike anion neighbors. Refinement of Cl occupancies indicated that approximately 3% of the column-anion sites are occupied by Cl_A, representing a Cl atom or a sequence of Cl atoms bounded by a vacancy in the anion column. In hexagonal ternary apatite, Cl thus occupies two sets of mirror-related sites about the mirror plane at $z = 1/4$ [Cl_B = $(0, 0, 0.37)$, $(0, 0, 0.13)$; Cl_A = $(0, 0, 0.44)$, $(0, 0, 0.06)$]; as Cl atoms are distributed equally

between the sites in each set, the locally monoclinic structure averages over the entire crystal to hexagonal symmetry.

Miscibility of F, Cl, and OH in hexagonal ternary apatite is thus a result of a Markovian anion sequence in the $[0, 0, z]$ anion columns. The Cl_B atom disordered below the mirror plane at $z = \frac{3}{4}$ (atom Cl in Fig. 2) cannot have an F atom [located at $(0, 0, \frac{1}{4})$] or OH disordered above the mirror plane at $z = \frac{1}{4}$ [located at $(0, 0, 0.30)$]; atom O(H) in Fig. 2] as a nearest column neighbor along $-c$. To change the chemical species in the sequence, the Cl atom must be adjacent to a OH ion disordered below the mirror plane at $z = \frac{1}{4}$ [at $(0, 0, 0.20)$], 2.96 Å distant. The F atoms can then be accommodated as neighbors of that OH ion, thus effecting ternary solution.

Monoclinic variants

Monoclinic apatite variants include end-member chlorapatite and hydroxylapatite that contain few or no "reversal sites" in the anion columns to bring about disorder. In these structures the OH and Cl ions are ordered into one of the two equivalent sites of their hexagonal counterparts, and thus monoclinic ($P2_1/b$) symmetry results (Hounslow and Chao, 1970; Mackie et al., 1972; Elliot et al., 1973). The monoclinic ternary apatite described here differs from these end-members in that all three column-anion species are accommodated in a previously unrecognized $P2_1/b$ variant. We present the general features of the structure; definition of finer details, such as disordering of the equivalents of hexagonal Ca(2), undoubtedly present as indicated by Ca thermal parameters and Ca(2)-Cl_b bond lengths, await more suitable crystals.

The positions of noncolumn atoms in $P2_1/b$ ternary apatite are similar to those in $P6_3/m$ ternary apatite (Table 6). The reduction of symmetry from hexagonal to monoclinic in ternary apatite results from ordering of the column anions into one of the two symmetry-equivalent column-anion sites present in hexagonal ternary apatite. Figure 3 depicts the correlation between column-anion sites in the two ternary structures.

In the monoclinic ternary apatite structure one position for Cl [Cl_A] exists near $(0, 0.25, 0.43)$, which is equivalent to the hexagonal position of $(0, 0, 0.43)$. The monoclinic ternary structure thus accommodates Cl_A in a position similar to one of the symmetry-equivalent Cl_A sites in hexagonal ternary apatite $[(0, 0, 0.44)]$. However, as in monoclinic chlorapatite, equivalent positions are no longer in the same column and related by mirrors but occur in neighboring columns and are related by b -glide planes.

A second position for chlorine (Cl_B) exists in monoclinic ternary apatite at $(0.00, 0.25, 0.13)$, which is equivalent to the hexagonal position of $(0, 0, 0.13)$. As shown previously, in hexagonal ternary apatite the majority of the chlorine atoms are located in the mirror-related Cl_B sites at $(0, 0, 0.37)$ and $(0, 0, 0.13)$. In monoclinic ternary apatite only one of these two sites is occupied in any given column.

In hexagonal ternary fluorapatite the F atoms occupy

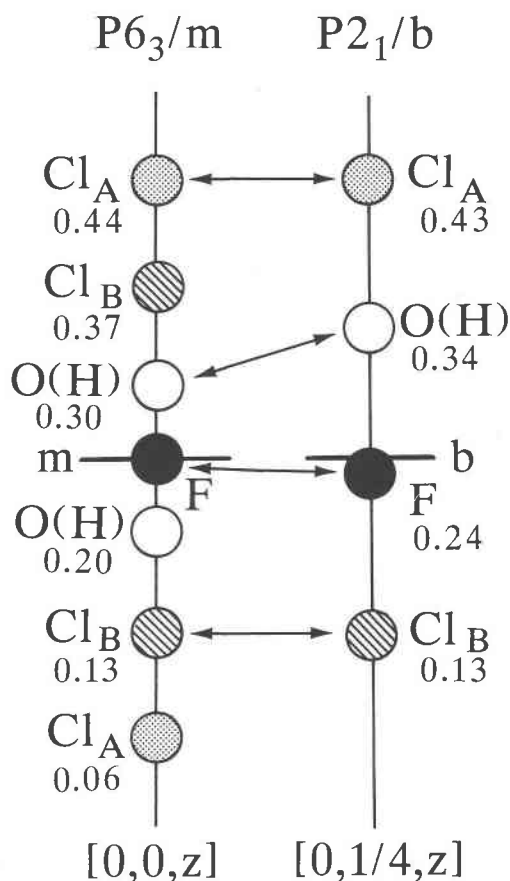


Fig. 3. Correlation of anion sites in $P6_3/m$ and $P2_1/b$ ternary apatites. Atoms represent possible anion sites associated with the mirror plane ($P6_3/m$) or the b -glide plane ($P2_1/b$) at $z = \frac{1}{4}$. Atom size is arbitrary, and the z positional parameter is given. The shift of the O(H) position between structures is largely a result of the difference in Cl content.

positions at the center of the Ca(2) triangles in the $2a$ special positions at $(0, 0, \frac{1}{4})$ and $(0, 0, \frac{3}{4})$, related by the 6_3 screw axis. In monoclinic ternary apatite the F atoms occupy similar positions [hexagonal equivalents = $(0, 0, 0.24)$ and $(0, 0, 0.74)$] related by the 2_1 axis.

In hexagonal ternary apatite OH is displaced from the mirror plane and half-occupies mirror-related sites at $(0, 0, 0.20)$ and $(0, 0, 0.30)$. The z parameter of OH, however, is sensitive to Cl content. Sudarsanan and Young (1978) demonstrated the covariance of z_{OH} and Cl content in apatites. Using their relationship, OH in apatite with 0.47 Cl atoms per formula unit (as in monoclinic ternary apatite) would be located near $(0, 0, 0.18)$ and $(0, 0, 0.32)$. In the monoclinic structure OH, like the Cl atoms, is ordered into one of these sites at $(0, 0.25, 0.34)$, which is equivalent to $(0, 0, 0.34)$ in hexagonal apatite.

The reduction of symmetry in monoclinic ternary apatite results from ordering of OH and Cl into one of the two equivalent hexagonal sites. It is not clear from this initial investigation what proportion of natural ternary

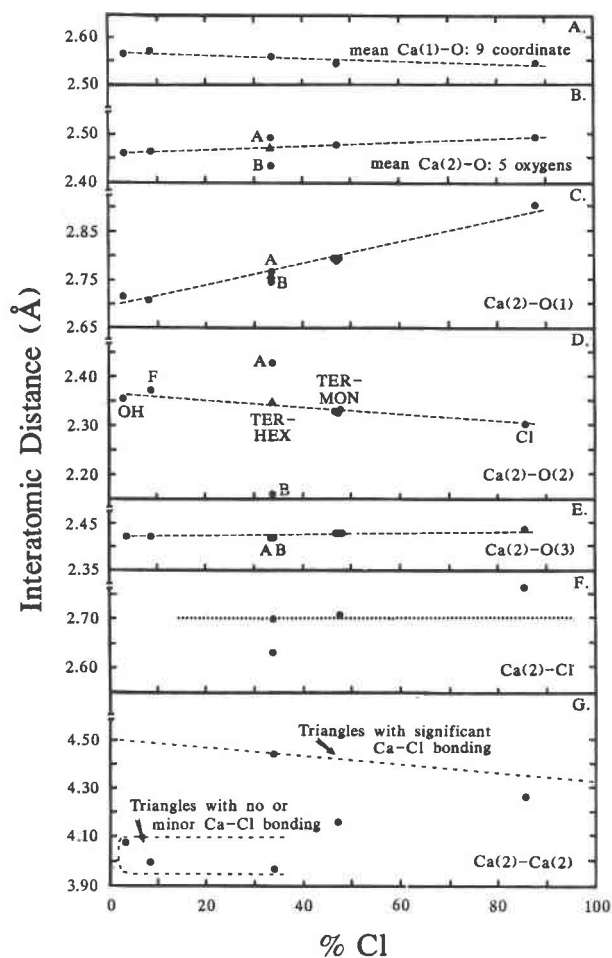


Fig. 4. Selected interatomic distances in natural F, Cl, OH ternary and end-member apatites. Ternary data (TER-HEX and TER-MON) are reported in this paper; end-member data (Cl, F, OH) are reported by Hughes et al. (1989). The data for ternary hexagonal apatite represented by triangles are interatomic distances for the average Ca(2) atom prior to refinement with a split-atom model; "A" and "B" in B, C, D, and E refer to split Ca(2) atoms. Dotted line at 2.7 Å in F included for reference; dashed line in G taken from Sudarsanan and Young (1978). See text for further discussion. Size of symbols is generally larger than ± 1 esd for each data point.

apatites possesses monoclinic symmetry, nor which physical or chemical conditions may result in monoclinicity in ternary (Cl, OH, F) species. The structures presented here, however, illustrate the unaddressed complexities in apatite crystal chemistry in that two crystals of similar composition differ in symmetry as a result of column-anion ordering.

CATION POLYHEDRA

The topological variations exhibited by cation polyhedra in both ternary apatites result from perturbations introduced by Cl atoms in the column-anion sites. Effects on interatomic distances in the P tetrahedron and the

Ca(1) polyhedron are minimal; however, variations within the Ca(2) polyhedron, which includes among its ligands the column anions, are regular and can be related to the Cl content.

Phosphate tetrahedra in both ternary structures have statistically identical mean P-O bond distances (1.532–1.533 Å). These values are identical, within ± 3 esd, to those observed for end-member fluor-, hydroxyl-, and chlorapatite (Hughes et al., 1989). Individual P-O bond distances and O-P-O angles are essentially constant with the exception of those involving O(3) atoms, which exhibit very small but systematic variations correlative with Cl content.

In both the ternary apatites discussed herein and in end-member phosphate apatites discussed by Hughes et al. (1989), Ca(1) bonds to three O(1) and three O(2) at short distances (~ 2.3 – 2.4 Å) and three O(3) at longer distances (~ 2.8 Å). Differences in interatomic distances among the five ternary and end-member structures are minor, although there is a slight tendency for the mean Ca(1)-O distances to decrease (~ 0.01 Å) with increasing Cl content (Fig. 4).

The Ca(2) polyhedron in phosphate apatites is an irregularly shaped polyhedron that is at least 6-coordinate [one O(2), four O(3), and one X column anion]. The coordination number may be larger if Ca(2) bonds to an O(1) atom or to an additional Cl atom. In hexagonal end-member apatites, the Ca(2) in the F and OH species is 7-coordinate if a long bond to O(1) (ca. 2.7 Å) is included in the coordination sphere, whereas in chlorapatite it is 8-coordinate if both O(1) (ca. 2.9 Å) and a weak bond to a second Cl atom are included. In the ternary hexagonal apatite reported in this study, Ca(2) is disordered into two sites, as discussed previously. The disordered Ca(2)_A position is similar to that recognized in the end-member apatite structures, with Ca(2)_A bonding to F, OH, and Cl_A at distances of ~ 2.29 , 2.32, and 2.63 Å, respectively. The atom in the Ca(2)_B position bonds to Cl_B, a unique Cl position recognized in ternary and Cl-bearing binary apatites. A similar disordering of Ca(2) is expected in the ternary monoclinic apatite based on the magnitude of the thermal parameters (Table 6), but the split atom was not modeled because of the lower quality of the data collected from the inferior monoclinic crystal.

Interatomic distances between Ca(2) and its ligands vary regularly with Cl content in the five apatites we have studied (this study and Hughes et al., 1989). The average of the four Ca(2)-O(3) bonds remains approximately constant at 2.42–2.43 Å (Fig. 4) in all of the structures. With increasing Cl content, the Ca(2)-O(2) bond decreases significantly, whereas the Ca(2)-O(1) distance increases significantly.

In a previous study of end-member hexagonal apatites, Hughes et al. (1989) interpreted the increase in the Ca(2)-O(1) distance in chlorapatite (vs. fluor- and hydroxylapatite) as a mechanism to reduce overbonding of Ca(2) that results from its coordination to a second Cl atom in the [001] column. In the ternary structures, it appears that the

Ca(2)-O(2) bonds may also contribute to the Ca(2) overbonding, as a significant decrease in Ca(2)-O(2) bond length occurs with increasing Cl content.

Refined Ca(2)-Cl distances in both ternary and end-member structures are close to the ideal value of ~ 2.7 Å. The short Ca(2)-Cl_B distance (~ 2.54 Å) reported in Table 7 for the monoclinic apatite is an artifact of the refinement procedure, as we did not model the Ca(2) split atoms. We expect that if Ca(2) were allowed to disorder in split-atom positions, readjustments in both Ca-Cl distances [Ca(2)_A-Cl_A; Ca(2)_B-Cl_B] would occur, and both would approach the ideal bond distance of ~ 2.7 Å.

The Ca(2) atoms are arranged in triangles that are centered around [001] containing the column anions. The size of these triangles can be related to the amount of Cl in an apatite structure and to the presence or absence of Ca-Cl bonds in a given Ca(2) triangle. The Ca(2)_A triangles bonded to the column anions OH, F, and Cl_A exist in an essentially Cl-free environment and exhibit similar Ca(2)-Ca(2) distances (~ 3.97 – 4.07 Å; Fig. 4). In contrast, the Ca(2)_B triangles in ternary apatite that involve significant Ca-Cl bonding [e.g., Ca(2)_B-Cl_B] exhibit a very regular inverse relationship between Ca(2)-Ca(2) distance and Cl content (Fig. 4). The latter relationship was first recognized by Sudarsanan and Young (1978) and was attributed by those authors to Ca-Cl bonding requirements.

IMPLICATIONS FOR BINARY Cl-F APATITES

Solid solution in ternary apatite is made possible by a 0.4 Å shift of the Cl atom relative to its position in end-member chlorapatite. The movement of the Cl 0.4 Å closer to the plane of Ca(2) atoms enables a OH neighbor to occupy a position at the next column anion site, at a distance of 2.96 Å. This configuration, however, does not permit a F ion as a neighbor to Cl in the anion column. It is thus not clear from the ternary structure how solid solution results in fluor-chlorapatite.

Using synthetic crystals, Mackie and Young (1974) addressed the incompatibility of F and Cl in apatite anion columns. They concluded that solid solution in pure F-Cl apatites is made possible by creation of new F sites in the anion column, which yields reasonable Cl-F distances. In preliminary refinements of natural, near-binary chlor-fluorapatite, we have found that small amounts of OH stabilize F in the 2a special position, and solid solution is made possible by splitting of the chlorine sites. The concentration of OH necessary to stabilize this Cl-F structure is not known; however, we are continuing experiments to elucidate the nature of solid solution in natural fluor-chlorapatites.

ACKNOWLEDGMENTS

We acknowledge Bart Kowallis of Brigham Young University and George Y. Chao of Carleton University for providing specimens for this study. Paul Robinson of Southern Illinois University kindly duplicated our experimental results for hexagonal apatite using a Rigaku Afcsc diffractometer. The National Science Foundation provided support for this project through grants EAR-8717655 and CHE-8418897 (J.M.H.), EAR-8517621 (K.D.C. and M.C.), and EAR-8916305 (J.M.H. and M.C.).

REFERENCES CITED

- Beevers, C.A., and McIntyre, D.B. (1946) The atomic structure of fluorapatite and its relation to that of tooth and bone material. *Mineralogical Magazine*, 27, 254–257.
- Boudreau, A.E., and McCallum, I.S. (1987) Halogens in apatites from the Stillwater Complex: Preliminary results (abs.). *EOS*, 68, 1518.
- Candela, P.A. (1986) Towards a thermodynamic model for the halogens in magmatic systems: An application to the melt-vapor-apatite equilibria. *Chemical Geology*, 57, 289–301.
- Crowley, K.D., and Cameron, M. (1987) Annealing of etchable fission-track damage in apatite: Effects of anion chemistry. *Geological Society of America Abstracts with Programs*, 19, 631–632.
- Crowley, K.D., Cameron, M., and McPherson, B.J. (1988) Annealing of etchable fission-track damage in F-, OH-, Cl-, and Sr-apatite: 1. Systematics and preliminary interpretations. *Proceedings of 6th International Fission Track Dating Conference, Besançon, France*.
- Elliot, J.C., Mackie, P.E., and Young, R.A. (1973) Monoclinic hydroxyapatite. *Science*, 180, 1055–1057.
- Exley, R.A., and Smith, J.V. (1982) The role of apatite in mantle enrichment processes and in the petrogenesis of some alkali basalt suites. *Geochimica et Cosmochimica Acta*, 46, 1375–1384.
- Frenz, B.A. (1985) Enraf-Nonius structure determination package. *SDP Users Guide (Version 4)*, Enraf-Nonius, Delft, The Netherlands.
- Green, P.F., Duddy, I.R., Gleadow, A.J.W., Tingate, P.R., and Laslett, G.M. (1986) Thermal annealing of fission tracks in apatite: 1. A qualitative description. *Chemical Geology*, 59, 237–253.
- Harrison, T.M., and Watson, E.B. (1984) The behavior of apatite during crustal anatexis: Equilibrium and kinetic considerations. *Geochimica et Cosmochimica Acta*, 48, 1467–1477.
- Henderson, P. (1984) Rare earth element geochemistry. Elsevier, Amsterdam.
- Hounslow, A.W., and Chao, G.Y. (1970) Monoclinic chlorapatite from Ontario. *Canadian Mineralogist*, 10, 252–259.
- Hughes, J.M., Cameron, M., and Crowley, K.D. (1989) Structural variations in natural F, OH, and Cl apatites. *American Mineralogist*, 74, 870–876.
- Mackie, P.E., Elliot, J.C., and Young, R.A. (1972) Monoclinic structure of synthetic Ca₅(PO₄)₃Cl, chlorapatite. *Acta Crystallographica*, B28, 1840–1848.
- Mackie, P.E., and Young, R.A. (1974) Fluorine-chlorine interaction in fluor-chlorapatite. *Journal of Solid State Chemistry*, 11, 319–329.
- Mehmel, M. (1930) Über die Struktur des Apatits: I. *Zeitschrift für Kristallographie*, 75, 323–331.
- Morrison, J., and Valley, J.W. (1989) Partitioning of F-Cl-OH between amphibole, apatite, and biotite in granulites from the Adirondack Mountains, New York (abs.). *EOS*, 70, 493.
- Náray-Szabó, S. (1930) The structure of apatite (CaF)Ca₄(PO₄)₆. *Zeitschrift für Kristallographie*, 75, 387–398.
- Nielson, D.R. (1988) Depositional environments and petrology of the Middle Jurassic Carmel Formation near Gunlock, Washington County, Utah, 108 p. M.S. thesis, Brigham Young University.
- Storner, J.C., and Carmichael, I.S.E. (1971) Fluorine-hydroxyl exchange in apatite and biotite: A potential igneous geothermometer. *Contributions to Mineralogy and Petrology*, 31, 121–131.
- Sudarsanan, K., and Young, R.A. (1978) Structural interactions of F, Cl, and OH in apatites. *Acta Crystallographica*, B34, 1401–1407.
- Sudarsanan, K., Young, R.A., and Wilson, A.J.C. (1977) The structures of some cadmium "apatites" Cd₂(MO₄)₂X: I. Determinations of the structures of Cd₂(VO₄)₂I, Cd₂(PO₄)₂Br, Cd₂(AsO₄)₂Br and Cd₂(VO₄)₂Br. *Acta Crystallographica*, B33, 3136–3142.
- Walker, N., and Stuart, D. (1983) An empirical method for correcting diffractometer data for absorption effects. *Acta Crystallographica*, A39, 158–166.
- Watson, E.B., Harrison, T.M., and Ryerson, F.J. (1985) Diffusion of Sm, Sr, and Pb in fluorapatite. *Geochimica et Cosmochimica Acta*, 49, 1813–1823.
- Weber, W.J., Wald, J.W., and Matske, H.J. (1985) Self-radiation in actinide host phases of nuclear waste forms. *Materials Research Society Symposium Proceedings*, 44, 679–686.

- Weber, W.J., and Roberts, F.P. (1983) A review of radiation effects in solid nuclear waste forms. *Nuclear Technology*, 60, 178–198.
- Wilson, A.J.C., Sudarsanan, K., and Young, R.A. (1977) The structures of some cadmium "apatites" $Cd_5(MO_4)_3X$: II. The distributions of the halogen atoms in $Cd_5(VO_4)_3I$, $Cd_5(PO_4)_3Br$, $Cd_5(AsO_4)_3Br$, $Cd_5(VO_4)_3Br$ and $Cd_5(PO_4)_3Cl$. *Acta Crystallographica*, B33, 3142–3154.
- Yardley, B.W.D. (1985) Apatite composition and the fugacities of HF and HCl in metamorphic fluids. *Mineralogical Magazine*, 49, 77–79.

MANUSCRIPT RECEIVED AUGUST 21, 1989

MANUSCRIPT ACCEPTED NOVEMBER 28, 1989